3610 *Inorg. Chem.* **2010**, *49*, 3610–3617
DOI: 10.1021/ic902062d

Inorganic Chemistry
Forum Article

Cytochrome P450: The Active Oxidant and Its Spectrum

Jonathan Rittle, Jarod M. Younker, and Michael T. Green*

Department of Chemistry, The Pennsylvania State University, University Park, Pennsylvania 16802

Received October 18, 2009

This Forum focuses on the nature of the elusive oxidizing intermediate in P450 catalysis. The identity of this species has reemerged as a topic of contentious debate. It was recently reported that laser flash photolysis (LFP) can be used to generate P450 compound I (P450-I) quantitatively. Kinetic analyses of the reaction of the LFP-generated intermediate with substrates have been suggested to indicate that compound I is not the active oxidant in P450 catalysis. We evaluate these claims via an analysis of the UV/visible spectrum of the LFP-generated intermediate. The techniques of singular value decomposition and target testing are used to obtain the spectrum of P450-I in a model-independent manner from stopped-flow data of the reaction of P450 with *m*-chloroperbenzoic acid. It is shown that the LFP-generated spectrum bears no similarity to the P450-I spectrum. One may conclude that the LFP-generated intermediate is not P450-I.

Introduction

Cytochrome P450 are a class of thiolate-ligated heme proteins that are involved in the production of hormones and the metabolism of xenobiotics.[1,2] Chemical interest in these systems stems from their ability to functionalize unactivated hydrocarbons.[2−5] P450s are known to insert an atom from molecular oxygen into a variety of organic substrates, often with high degrees of regio- and stereoselectivity. The C−H bonds hydroxylated by P450s form a ubiquitous and rather unreactive moiety in organic chemistry. Synthetic catalysts that could selectively functionalize them would revolutionize organic synthesis.

This Forum examines the nature of the elusive oxidizing-intermediate in P450 catalysis (Figure 1). The identity of this species has reemerged as a topic of contentious debate. It was recently reported that laser flash photolysis (LFP) can be used, in conjunction with peroxynitrite (PN), to generate P450 compound I (P450-I) quantitatively.[6,7] Kinetic analyses of the reaction of the LFP-generated intermediate with substrates have been suggested to indicate that compound I is not the active oxidant in P450 catalysis.[6,8,9]

Despite claims of exceedingly long lifetimes ($t_{1/2} > 10$ min),[6,7] the LFP-generated intermediate has only been characterized with UV/visible spectroscopy.[6−11] The spectrum of the LFP-generated intermediate is dramatically different from the P450-I spectrum obtained from stopped-flow reactions of P450 with *m*-chloroperbenzoic acid (*m*CPBA).[12,13] It has been suggested that the reason for this discrepancy lies in the improper use of the global analysis fitting routines that are required to extract the P450-I spectrum from a stopped-flow data set.[8] It has been argued that the solutions obtained from global analysis are highly dependent upon the initial guess for rate constants.[8]

In what follows, we briefly review evidence implicating compound I in substrate oxidation. We then discuss the recent claims of P450-I generation using LFP, detailing attributes of the putative P450-I spectrum obtained via this technique. Finally, we present two model-independent methods for obtaining the spectrum of P450-I from stopped-flow data: no guesses or assumptions about reaction kinetics are made or required. The P450-I spectrum obtained by these methods bears no resemblance to the spectrum of the LFP-generated intermediate, but it is remarkably similar to P450-I

*To whom correspondence should be addressed. E-mail: mtg10@psu.edu.

(1) de Montellano, P. R. O. *Cytochrome P450 Structure, Mechanism, and Biochemistry*, 3rd ed.; Kluwer Academic/Plenum Publishers: New York, 2005.
(2) de Montellano, P. R. O. *Chem. Rev.* **2010**, *110*, 932−948.
(3) Stevenson, J. A.; Westlake, A. C. G.; Whittock, C.; Wong, L. L. *J. Am. Chem. Soc.* **1996**, *118*, 12846–12847.
(4) Koo, L. S.; Immoos, C. E.; Cohen, M. S.; Farmer, P. J.; de Montellano, P. R. O. *J. Am. Chem. Soc.* **2002**, *124*, 5684–5691.
(5) Groves, J. T.; Mcclusky, G. A.; White, R. E.; Coon, M. J. *Biochem. Biophys. Res. Commun.* **1978**, *81*, 154–160.
(6) Wang, Q.; Sheng, X.; Horner, J. H.; Newcomb, M. *J. Am. Chem. Soc.* **2009**, *131*, 10629–10636.
(7) Yuan, X. T.; Wang, Q.; Horner, J. H.; Sheng, X.; Newcomb, M. *Biochemistry* **2009**, *48*, 9140–9146.
(8) Sheng, X.; Horner, J. H.; Newcomb, M. *J. Am. Chem. Soc.* **2008**, *130*, 13310–13320.
(9) Sheng, X.; Zhang, H. M.; Im, S. C.; Horner, J. H.; Waskell, L.; Hollenberg, P. F.; Newcomb, M. *J. Am. Chem. Soc.* **2009**, *131*, 2971–2976.
(10) Newcomb, M.; Zhang, R.; Chandrasena, R. E. P.; Halgrimson, J. A.; Horner, J. H.; Makris, T. M.; Sligar, S. G. *J. Am. Chem. Soc.* **2006**, *128*, 4580–4581.
(11) Sheng, X.; Zhang, H. M.; Hollenberg, P. F.; Newcomb, M. *Biochemistry* **2009**, *48*, 1620–1627.
(12) Egawa, T.; Shimada, H.; Ishimura, Y. *Biochem. Biophys. Res. Commun.* **1994**, *201*, 1464–1469.
(13) Kellner, D. G.; Hung, S. C.; Weiss, K. E.; Sligar, S. G. *J. Biol. Chem.* **2002**, *277*, 9641–9644.

 Published on Web 04/12/2010

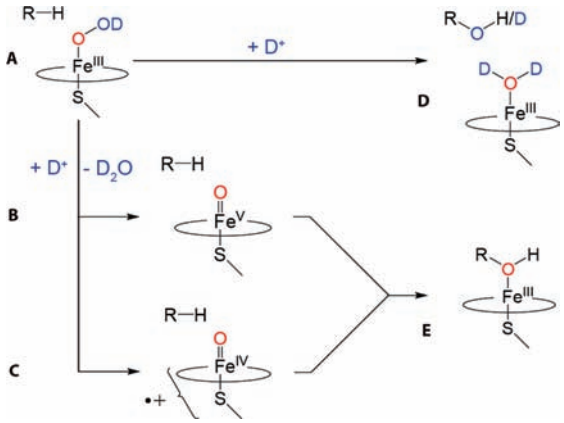

Figure 1. Species that have been proposed to play a role in P450 oxidations and their product states: (A) ferric hydroperoxo complex; (B) perferryl state; (C) compound I; (D) product expected if oxidation is performed by ferric hydroperoxo; (E) product expected for iron−oxo oxidations.

spectra obtained from previous stopped-flow investigations as well as the spectrum of chloroperoxidase compound I (CPO-I).

Evidence for the Role of Compound I in Substrate Hydroxylations. Descriptions of the full catalytic cycle of cytochrome P450 can be found in a number of reviews on the subject.[1,2] Here we focus only on those species that have been postulated to play an active role in substrate hydroxylations. Our examination starts with the last well-characterized intermediate in the catalytic cycle, the ferric hydroperoxo complex (shown as part A in Figure 1). This species is capable of epoxidation,[14−16] but it does not appear to be the active hydroxylating species in P450.[16,17] In the generally accepted mechanism for substrate hydroxylation, this species protonates at the distal oxygen to lose water and form compound I (see part C in Figure 1).[1,17]

Compound I is an iron(IV) oxo species with an additional oxidizing equivalent delocalized over the porphyrin and thiolate ligands. This species has, for the most part, eluded spectroscopic detection. It is not seen under normal turnover conditions, but it can be generated with peroxides in stopped-flow experiments. Three groups have reported the production of P450-I using *m*CPBA as an oxidant.[12,13,18] In each case, the intermediate was prepared in low yield and the reported spectrum of P450-I was obtained via the use of singular value decomposition (SVD) and global analysis techniques.[19,20] Spectral assignments of P450-I were based, in part, on comparisons with chloroperoxidase (CPO). CPO is a thiolate-ligated heme enzyme that is known to hydroxylate activated hydrocarbons.[21−23] The high-valent forms of CPO are electronically equivalent to those of P450, but they can be prepared and isolated in high yield, allowing characterization by a number of spectroscopies.[24−32] As a result, CPO has served as an important model system in the study of P450 chemistry.

On the basis of large kinetic isotope effects and the retention of stereochemistry at the oxidized carbon, Groves and co-workers proposed the "rebound mechanism" for substrate hydroxylations in P450.[5,33] In what has become the consensus hydroxylation mechanism, compound I abstracts hydrogen from the substrate to form an iron(IV) hydroxide species that rapidly recombines with the substrate radical to form hydroxylated product.

Indications that the active oxidant is an iron oxo species (as opposed to the ferric hydroperoxo complex) have come from work on mutant enzymes that lack a highly conserved threonine in the distal pocket. T → A mutants of $P450_{cam}$ do not hydroxylate camphor but will accept electrons and convert dioxygen to peroxide (uncoupling).[34,35] Experiments have shown that the threonine plays an important role in oxygen activation. The residue is adjacent to the dioxygen binding site, and it controls the delivery of the final proton in the catalytic cycle. By directing protonation at the distal oxygen, the conserved threonine promotes heterolytic scission of the O−O bond and iron oxo formation. Insight into the role of the threonine was obtained through cryogenic radiolytic−reduction experiments.[36] In these experiments, ferrous oxy P450 was reduced at 77 K to form the hydroperoxo species in both mutant and wild-type enzymes.[17,37] In both systems, the hydroperoxo species is stable at 77 K. However, upon annealing at higher temperatures (∼220 K), the wild-type enzyme quantitatively and stereospecifically hydroxylates substrate, while the T → A mutant reverts to ferric enzyme without product formation. These experiments indicated that the hydroperoxo complex is not a competent hydroxylating species in $P450_{cam}$.

(14) Vaz, A. D. N.; McGinnity, D. F.; Zarehbin-Irani, P.; Coon, M. J.; Salaun, J. P.; Koop, D. R.; Klopfenstein, B. *FASEB J.* **1997**, *11*, A807–A807.
(15) Vaz, A. D. N.; McGinnity, D. F.; Coon, M. J. *Proc. Natl. Acad. Sci. U.S.A.* **1998**, *95*, 3555–3560.
(16) Jin, S. X.; Makris, T. M.; Bryson, T. A.; Sligar, S. G.; Dawson, J. H. *J. Am. Chem. Soc.* **2003**, *125*, 3406–3407.
(17) Davydov, R.; Makris, T. M.; Kofman, V.; Werst, D. E.; Sligar, S. G.; Hoffman, B. M. *J. Am. Chem. Soc.* **2001**, *123*, 1403–1415.
(18) Spolitak, T.; Dawson, J. H.; Ballou, D. P. *J. Biol. Chem.* **2005**, *280*, 20300–20309.
(19) Malinowski, E. R. *Factor Analysis in Chemistry*, 3rd ed.; Wiley-Interscience: New York, 2002.
(20) Maeder, M.; Zuberbuhler, A. D. *Anal. Chem.* **1990**, *62*, 2220–2224.
(21) van Rantwijk, F.; Sheldon, R. A. *Curr. Opin. Biotechnol.* **2000**, *11*, 554–564.
(22) Zaks, A.; Dodds, D. R. *J. Am. Chem. Soc.* **1995**, *117*, 10419–10424.
(23) Hu, S. H.; Hager, L. P. *J. Am. Chem. Soc.* **1999**, *121*, 872–873.
(24) Stone, K. L.; Behan, R. K.; Green, M. T. *Proc. Natl. Acad. Sci. U.S.A.* **2006**, *103*, 12307–12310.
(25) Stone, K. L.; Hoffart, L. M.; Behan, R. K.; Krebs, C.; Green, M. T. *J. Am. Chem. Soc.* **2006**, *128*, 6147–6153.
(26) Stone, K. L.; Behan, R. K.; Green, M. T. *Proc. Natl. Acad. Sci. U.S.A.* **2005**, *102*, 16563–16565.
(27) Green, M. T.; Dawson, J. H.; Gray, H. B. *Science* **2004**, *304*, 1653–1656.
(28) Rutter, R.; Hager, L. P.; Dhonau, H.; Hendrich, M.; Valentine, M.; Debrunner, P. *Biochemistry* **1984**, *23*, 6809–6816.
(29) Egawa, T.; Proshlyakov, D. A.; Miki, H.; Makino, R.; Ogura, T.; Kitagawa, T.; Ishimura, Y. *J. Biol. Inorg. Chem.* **2001**, *6*, 46–54.
(30) Egawa, T.; Miki, H.; Ogura, T.; Makino, R.; Ishimura, Y.; Kitagawa, T. *FEBS Lett.* **1992**, *305*, 206–208.
(31) Schunemann, V.; Jung, C.; Terner, J.; Trautwein, A. X.; Weiss, R. *J. Inorg. Biochem.* **2002**, *91*, 586–596.
(32) Hosten, C. M.; Sullivan, A. M.; Palaniappan, V.; Fitzgerald, M. M.; Terner, J. *J. Biol. Chem.* **1994**, *269*, 13966–13978.
(33) Groves, J. T.; Mcclusky, G. A. *J. Am. Chem. Soc.* **1976**, *98*, 859–861.
(34) Martinis, S. A.; Atkins, W. M.; Stayton, P. S.; Sligar, S. G. *J. Am. Chem. Soc.* **1989**, *111*, 9252–9253.
(35) Imai, M.; Shimada, H.; Watanabe, Y.; Matsushimahibiya, Y.; Makino, R.; Koga, H.; Horiuchi, T.; Ishimura, Y. *Proc. Natl. Acad. Sci. U.S.A.* **1989**, *86*, 7823–7827.
(36) Davydov, R.; Hoffman, B. M.; Valentine, A. M.; Lippard, S. J.; Sligar, S. G.; Ikeda-Saito, M. *J. Inorg. Biochem.* **1999**, *74*, 110–110.
(37) Davydov, R.; Macdonald, I. D. G.; Makris, T. M.; Sligar, S. G.; Hoffman, B. M. *J. Am. Chem. Soc.* **1999**, *121*, 10654–10655.

Evidence for the involvement of an iron oxo species in wild-type hydroxylations comes from the fact that (1) the first detectable product state contains hydroxycamphor bound to ferric iron and (2) the hydroxyl proton originates from camphor (see part E in Figure 1). Hydroxylation by a ferric hydroperoxo species would be expected to yield a water-coordinated heme and a scrambled hydroxyl proton (see part D in Figure 1).

Perferryl State. Compound I is generally accepted to be the hydroxylating intermediate in P450 chemistry. However, compound I has not been observed under normal turnover conditions. Also, the transient nature of the intermediate has precluded reactivity studies in which P450-I generated with peroxides could be subsequently reacted with substrates.

Recently, Newcomb and co-workers have presented a method for preparing compound I in high yield.[10] In a series of investigations, they have discussed the use of LFP as a tool to generate compound I from ferryl species (i.e., compound II).[6−11] It has been reported that LFP allows the quantitative production of P450-I.[6,7]

Reactivity studies with the LFP-generated species have resulted in a controversial proposal. It has been suggested that compound I is not the active oxidant in P450.[6,8,9] These studies hint at the existence of a perferryl state that precedes compound I formation.[6,8−10] It is suggested that this iron(V) oxo intermediate (see part B in Figure 1) could be the oxidizing species in P450 chemistry.

Newcomb and co-workers' controversial results depend upon the ability to create P450-I via LFP. Except for UV/visible data (which is the focus of this Forum), no spectroscopic evidence for the existence of LFP-generated P450-I has been reported. The generation of P450-I requires the production of P450 compound II (P450-II). Newcomb's group has employed the reaction of PN with P450 to accomplish this task.[6−11,38] The production of compound II by this pathway is not uncontroversial. There is evidence that the reaction of PN with P450s yields a ferric nitrosyl complex.[39] The generation of compound I from such a species is clearly problematic.

The reported spectrum of LFP-generated P450-I is unlike the P450-I spectra reported previously by Sligar and Egawa.[12,13] The LFP-generated P450-I spectrum looks remarkably similar to that of ferric enzyme.[6,7] Newcomb and co-workers notes that the Soret bands of the LFP-generated species are centered at the same wavelengths as those of ferric enzyme and that only small intensity changes accompany quantitative conversion between the two (see Figure 1 of ref 6).[6,7] They suggest that the similarity between the spectra has been a major obstacle in detecting compound I under turnover conditions.

The P450-I spectra reported by Sligar and Egawa were obtained from the reaction of P450 with peroxides. These spectra show great similarity to the well-known spectrum of CPO-I.[40] In both cases, the P450-I spectra were obtained from stopped-flow reaction data using the technique of global analysis (see below).[12,13] Newcomb and co-workers have criticized these results, suggesting that the spectra obtained were biased by knowledge of the CPO-I spectrum.[8] They report that global analysis of *m*CPBA−P450 reaction data provides a series of solutions that are dependent upon the initial guess for rate constants.[8] They suggest that, in efforts to obtain spectra that resemble CPO-I, previous investigations have chosen solutions with rate constants that are too large. Sligar and co-workers report a compound I decay rate of $k = 29.4\ s^{-1}$ (in the absence of a substrate, at pH 7 and 4 °C), while Newcomb's group indicates that $k = 2.3\ s^{-1}$ is more appropriate.[8,13]

Newcomb's controversial results hinge upon two events: (1) the production of P450-II via the reaction of P450 with PN and (2) the creation of P450-I via LFP of P450-II. The reaction of PN with P450s has been addressed previously.[39] In what follows, we evaluate the latter claim by comparing the spectrum of the LFP-generated intermediate to the spectrum of P450-I obtained from the reaction with *m*CPBA. Importantly, the P450-I spectrum used for comparison is generated by model-independent techniques that require no assumptions about kinetics.

UV/Visible Spectrum of P450-I. To provide some perspective on the UV/visible spectrum of P450-I, we present an analysis involving SVD of the time-dependent data obtained during the reaction of peroxides with CPO and CYP119, the thermophillic P450 from *Sulfolobus acidocaldarius*.[41−43] (see the Experimental Section for details on the reaction conditions). Before we examine the data, we provide a brief introduction to the methods involved and refer those interested in more detail to a number of advanced treatments of the subject.[19,44−50]

SVD is a linear algebraic technique that can allow one to determine the number of important factors (i.e., chemical species) that are involved in a reaction.[19,44,45] The technique involves diagonalization of the covariance matrix, which is simply the data matrix multiplied by its transpose (eq 1).

$$\mathbf{Z} = \mathbf{D}^{\mathrm{T}}\mathbf{D} \tag{1}$$

where $\mathbf{Z}$ is the covariance matrix and $\mathbf{D}$ is the $m \times r$ data matrix, which for stopped-flow data contains r absorption spectra, each with m data points. Spectra taken at different time points form the columns of $\mathbf{D}$.

The eigenvalues obtained from this diagonalization are, by definition, the square of the singular values (for

(38) Newcomb, M.; Halgrimson, J. A.; Horner, J. H.; Wasinger, E. C.; Chen, L. X.; Sligar, S. G. *Proc. Natl. Acad. Sci. U.S.A.* **2008**, *105*, 8179–8184.
(39) Behan, R. K.; Hoffart, L. M.; Stone, K. L.; Krebs, C.; Green, M. T. *J. Am. Chem. Soc.* **2007**, *129*, 5855–5859.
(40) Palcic, M. M.; Rutter, R.; Araiso, T.; Hager, L. P.; Dunford, H. B. *Biochem. Biophys. Res. Commun.* **1980**, *94*, 1123–1127.
(41) Wright, R. L.; Harris, K.; Solow, B.; White, R. H.; Kennelly, P. J. *FEBS Lett.* **1996**, *384*, 235–239.
(42) McLean, M. A.; Maves, S. A.; Weiss, K. E.; Krepich, S.; Sligar, S. G. *Biochem. Biophys. Res. Commun.* **1998**, *252*, 166–172.
(43) Rabe, K. S.; Kiko, K.; Niemeyer, C. M. *ChemBioChem* **2008**, *9*, 420–425.
(44) Malinowski, E. R. *Anal. Chem.* **1977**, *49*, 612–617.
(45) Johnson, R. A.; Wichern, D. W. *Applied Multivariate Statistical Analysis*, 2nd ed.; Prentice-Hall: Englewood Cliffs, NJ, 1988.
(46) Brayden, T. H.; Poropatic, P. A.; Watanabe, J. L. *Anal. Chem.* **1988**, *60*, 1154–1158.
(47) Carvalho, A. R.; Wattoom, J.; Zhu, L. F.; Brereton, R. G. *Analyst* **2006**, *131*, 90–97.
(48) Little, R. J. A.; Rubin, D. B. *Statistical Analysis with Missing Data*; Wiley: New York, 1987.
(49) Lorber, A.; Kowalski, B. R. *Anal. Chem.* **1989**, *61*, 1168–1169.
(50) Malinowski, E. R.; Mccue, M. *Anal. Chem.* **1977**, *49*, 284–287.

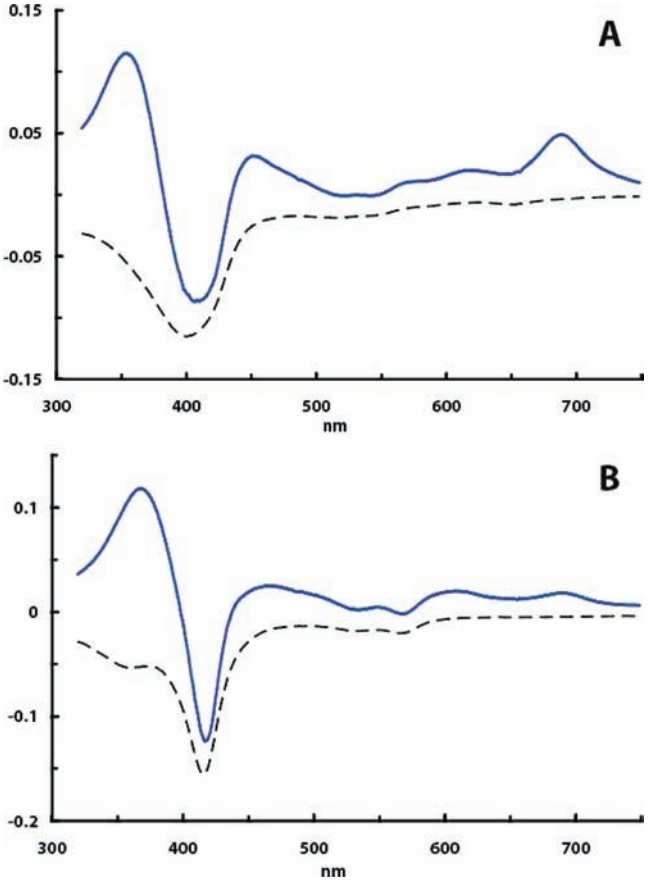

Figure 2. Abstract spectra obtained from SVD of stopped-flow data for (A) the reaction of CPO with peracetic acid and (B) the reaction of CYP119 with *m*CPBA. See the Experimental Section for the reaction conditions.

which the technique is named). The nature of the eigenvectors depends on the data set. For stopped-flow data, the eigenvectors obtained are either abstract absorption spectra or abstract concentration profiles. Whether one obtains abstract spectra or concentration profiles depends upon the order in which the data matrix and its transpose are multiplied, $\mathbf{Z} = \mathbf{D}\mathbf{D}^{\mathrm{T}}$ or $\mathbf{D}^{\mathrm{T}}\mathbf{D}$, respectively. Both sets of abstract eigenvectors form orthonormal bases that can be used with the singular values (which are independent of the order of multiplication) to reconstruct the data (eq 2).

$$\mathbf{D} = \mathbf{U}\mathbf{S}\mathbf{V}^{\mathrm{T}} \tag{2}$$

where $\mathbf{D}$ is the data matrix, $\mathbf{U}$ is a $m \times n$ matrix containing n spectral eigenvectors in columns, $\mathbf{S}$ is a $n \times n$ square-diagonal matrix containing n singular values, and $\mathbf{V}^{\mathrm{T}}$ is a $n \times r$ matrix containing n concentration vectors in rows.

The vectors obtained from diagonalization of the covariance matrix are called abstract because they do not represent individual chemical species but are linear combinations of the real concentration profiles and spectra. As a result, both the abstract spectra and concentration profiles may have negative values. Figure 2 provides examples of abstract absorption spectra. Abstract concentration profiles can be found in the Supporting Information.

By examination of the singular values, one may determine the number of species involved in a reaction. For "perfect noiseless data", the number of nonzero singular values equals the number of UV/visible absorbing species in the reaction. Real data will have noise, and this noise will result in additional singular values, which are small but nonzero. By omitting these values from the reconstruction, one can reduce the noise in the data set. Small singular values may also be an indication of a fleeting intermediate that contributes little to the data set. There are statistical tests that can be coupled with SVD to aid in the determination of the number of significant singular values.[19,44] However, a visual inspection of the abstract vectors and singular values is usually sufficient.

Of course, what one seeks are not singular values or abstract vectors. What one wants are the real and chemically meaningful spectra and concentration profiles. Remember that the abstract vectors are just linear combinations of the real vectors. Thus, the real vectors may be obtained from an appropriate linear combination (i.e., a rotation) of the abstract vectors (eqs 3−5). The problem is that the matrix $\mathbf{R}$ that accomplishes this rotation is generally unknown.

$$\mathbf{D} = \mathbf{U}\mathbf{R}^{-1}\mathbf{R}\mathbf{S}\mathbf{V}^{\mathrm{T}} \tag{3}$$

$$\mathbf{D} = (\mathbf{U}\mathbf{R}^{-1})(\mathbf{R}\mathbf{S}\mathbf{V}^{\mathrm{T}}) \tag{4}$$

$$\mathbf{D} = \boldsymbol{\varepsilon}_{\mathrm{real}}\mathbf{C}_{\mathrm{real}} \tag{5}$$

where $\mathbf{R}$ is the rotation matrix, $\boldsymbol{\varepsilon}_{\mathrm{real}}$ is an $m \times n$ matrix containing n real extinction coefficients in columns, and $\mathbf{C}_{\mathrm{real}}$ is an $n \times r$ matrix containing n real concentration profiles in rows.

One technique that chemists can use to determine the appropriate rotation matrix is global analysis.[20] Global analysis is a model-dependent means of determining spectra, concentration profiles, and rate constants. The method was used by Egawa and Sligar to obtain their reported P450-I spectra. It works in the following way: One first assumes a model (mechanism) for the chemical reaction. For example, in the reactions of CPO and CYP119 with peroxides, one might assume a second-order formation of compound I followed by a first-order decay back to ferric enzyme (eq 6).

$$\mathrm{CYP119} + m\mathrm{CPBA} \xrightarrow{k_1} \mathrm{CYP119\text{-}I} \xrightarrow{k_2} \mathrm{CYP119} \tag{6}$$

Initial guesses for the rate constants (k_1 and k_2) are then used to generate initial-guess concentration profiles via the chemical rate equations. Because both the real (initial-guess) and abstract concentration profiles are known, the rotation matrix that connects these two bases can be determined and applied to the abstract spectra to generate the real (initial-guess) spectra. These spectra and profiles are then used to generate a data matrix (eq 5). The difference between this matrix and the actual data matrix (the residual) is then minimized by varying the rate constants.

Assuming one has chosen the appropriate model, minimization of the residual ideally yields a solution with the correct spectra, concentration profiles, and rate constants for the reaction. In practice, however, noise in the data (and complexity in the model) may result in a number of fits (minima) with similar fit quality. Only one of these solutions is correct, and the alternative fits yield incorrect rate constants, spectra, and concentration profiles. These incorrect spectra and concentration profiles are still linear combinations of the abstract vectors. They are just not the right linear combinations. Newcomb and co-workers report obtaining a number of these solutions in their examinations of the reaction of CYP119 with *m*CPBA. These alternative solutions form an important component of their criticism of the CYP119-I spectrum reported by Sligar.

Fortunately, the situation can be made much easier when only two absorbing species are involved. If the spectrum of one of these species (say ferric enzyme) is known exactly, as is the case in the reaction of CPO and CYP119 with peroxides, then the second unknown spectrum (i.e., compound I) may be obtained by combining the abstract spectra in such a way as to remove all contributions originating from the known spectrum. An analysis of the singular values and abstract eigenvectors indicates that only two species contribute significantly to the CPO and CYP119 data sets. The first four singular values are 104.6, 5.16, 0.08, and 0.05 for CPO and 92, 2.81, 0.06, and 0.05 for CYP119. Figure 2 shows the abstract spectra corresponding to the first two singular values for each data set. The abstract concentration profiles and additional spectra can be found in the Supporting Information.

The abstract spectra of the CPO and CYP119 reactions are remarkably similar. There are minor variations in the widths and positions of bands that reflect the fact that ferric CPO is high-spin, while ferric CYP119 is low-spin, but overall the resemblance is striking. In both cases, there is one spectrum that looks predominantly like an inverted (i.e., negative) ferric spectrum and another that resembles a difference spectrum of ferric and compound I. In both cases, the "difference" spectrum shows features (Soret bands around 400−420 nm and Q bands around 520−570 nm) that are clearly associated with ferric enzyme. To obtain the compound I spectrum, all that one needs to do is to combine these abstract spectra together to minimize the ferric features. This process is illustrated in Figure 3.

The spectra shown in black in Figure 3 are the ferric forms of CPO (top) and CYP119 (bottom). The other three spectra are different combinations of the abstract vectors shown in Figure 2. The combinations shown with dotted lines have a negative ferric component. They have holes (inverted regions) in the Soret- and Q-band regions associated with ferric enzyme. In contrast, the combinations shown with dashed lines have a positive ferric component. One can see peaks that correspond to the ferric Soret and Q bands. The combinations shown in red lack features associated with ferric enzyme: these are the compound I spectra. The spectrum obtained for CPO is in excellent agreement with the well-known spectrum of CPO-I, and the CYP119-I spectrum obtained by this method bears great similarity to the spectrum reported

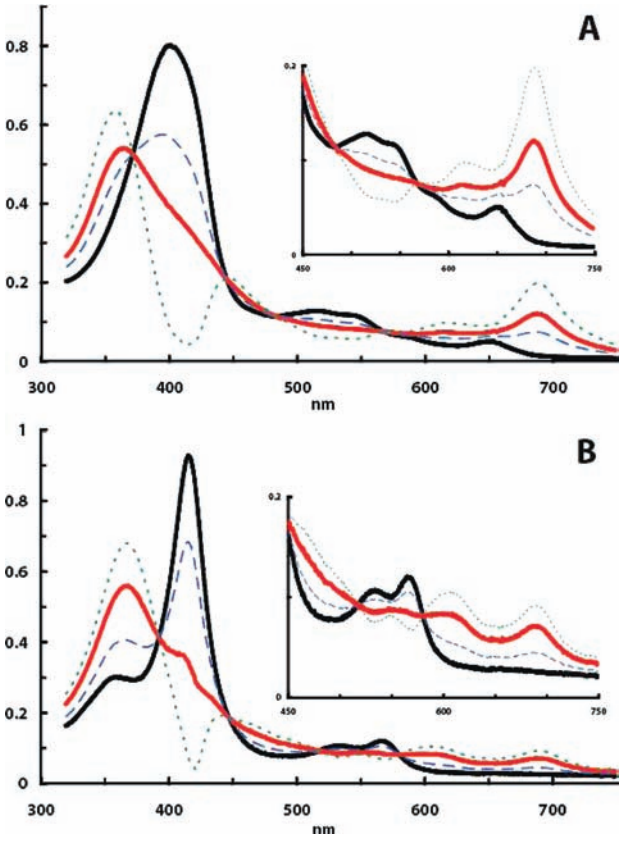

Figure 3. Compound I spectrum obtained from linear combinations of abstract spectra for (A) CPO and (B) CYP119. Ferric spectra are shown in black for comparison. The other spectra are linear combinations of the abstract spectra shown in Figure 2. Spectra shown with dotted lines have a negative ferric component. Spectra shown with dashed lines have a positive ferric component. The combinations shown in red lack features associated with ferric enzyme: these are the compound I spectra.

by Sligar. This method of generating the compound I spectra is model-independent (no rate law was assumed), but it does require some user input. One must visually determine the appropriate combination of the abstract vectors.

A model-independent method that requires no user input is target testing.[19,46−50] In this method, one uses the abstract vectors to create a projection operator (eq 7) that can be applied to candidate spectra to determine if the species belonging to the spectra are involved in the reaction (eq 8).

$$\mathbf{P} = \mathbf{U}\mathbf{U}^{\mathrm{T}} \tag{7}$$

$$\mathbf{Y} = \mathbf{P}\mathbf{X} \tag{8}$$

Here **X** is the input or targeted vector and **Y** is the vector returned. If target testing returns the input spectrum (i.e., **Y** = **X**), it means one of two things: (1) the targeted species, **X**, is in the reaction or (2) species in the reaction have spectra that can be added together to yield the target spectrum. The second of these scenarios is highly unlikely for the systems of interest. The reason is that it is improbable that the spectra of any number of enzymatic states for a given system will add together to yield the spectrum of an additional distinct species. Think of the

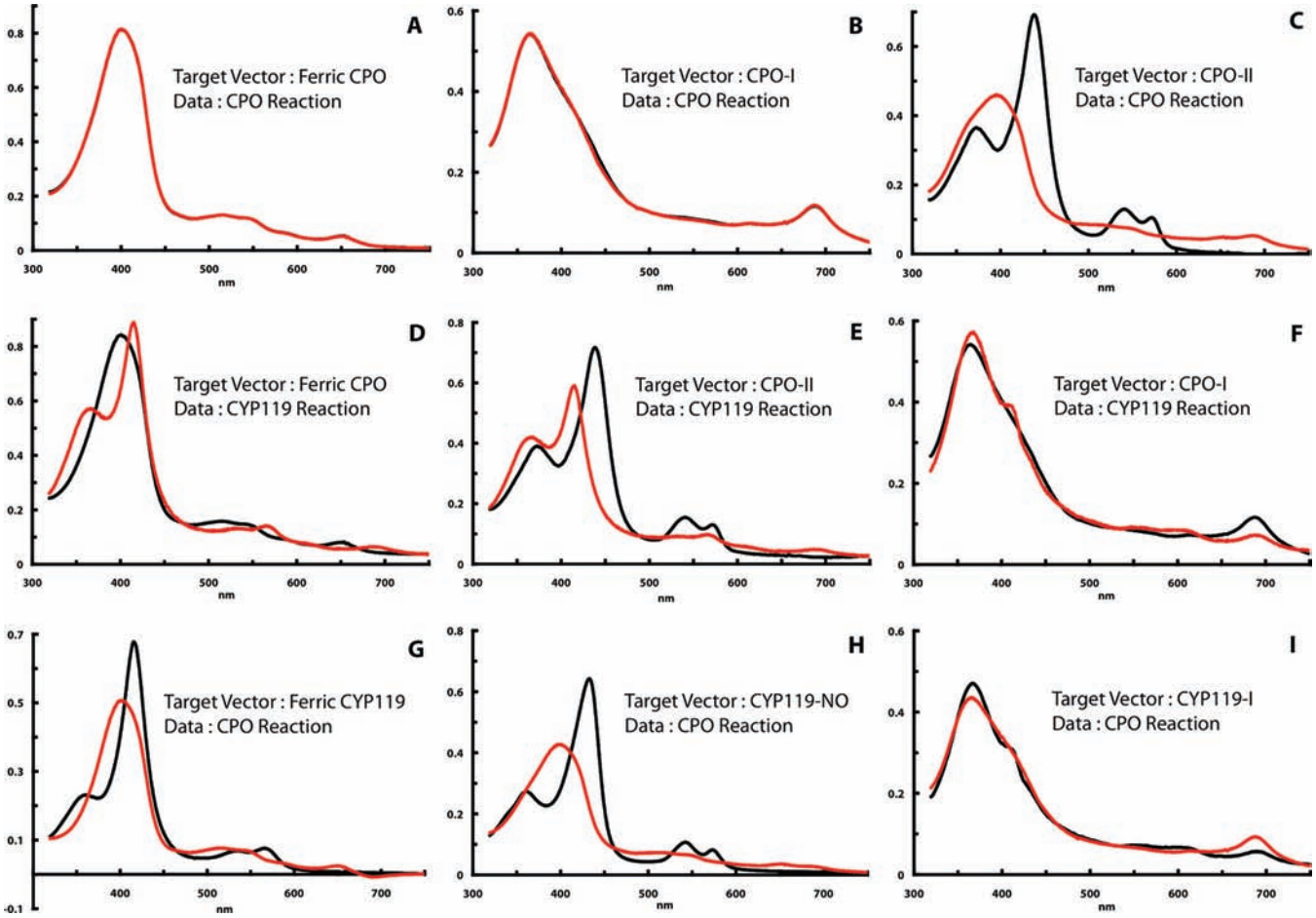

Figure 4. Target testing for CPO and CYP119 data sets. In each case, the targeted spectrum is shown in black and the spectrum returned is in red. The targeted vector and data set (vector:data) are (A) CPO:CPO, (B) CPO-I:CPO, (C) CPO-II:CPO, (D) CPO:CYP119, (E) CPO-II:CYP119, (F) CPO-I:CYP119, (G) CYP119:CPO, (H) CYP119-NO:CPO, and (I) CYP119-I:CPO. See the Experimental Section for details on the reaction conditions.

various forms of P450: high-spin ferric, low-spin ferric, ferrous, ferrous oxy, ferrous CO, ferric NO, and ferric hydroperoxy. Can the spectra of any number of these be combined in a way to produce another member of the set?

In Figure 4, panels A−C illustrate the application of target testing on the reaction of CPO with peracetic acid. They show the results obtained from target testing the spectra of ferric CPO, CPO-I, and CPO-II on the CPO data set. Analysis of the singular values indicates only two species in the reaction. These are ferric CPO and CPO-I. As shown in panels A and B, target testing the spectra of these species returns essentially perfect copies. The situation is quite different for the spectrum of CPO-II. Target testing does not return anything remotely similar to the CPO-II spectrum, a clear indication that CPO-II is not a significant component in the CPO data set.

The application of target testing outlined above is the classical application of the technique. To address the question of the UV/visible spectrum of CYP119-I, we adapt the technique and apply it in a nontraditional manner. To obtain an approximation for the spectrum of CYP119-I, we target test the CYP119 data set with the spectrum of CPO-I. The abstract vectors obtained for the CPO and CYP119 data sets are different (Figure 2): they do not span the same space. As a result, we do not expect a carbon copy of CPO-I to come out of the testing. What we do expect to obtain, however, is the closest analogue in the space spanned by the CYP119 vectors (i.e., CYP119-I). The logic is as follows. The ligands surrounding iron in the active sites of CPO-I and P450-I are identical. We thus make the chemically intuitive assumption that the spectra of these complexes should be similar. By target testing CPO-I on the CYP119 data set, we return the closest approximation to CPO-I that one can make with the abstract vectors of the CYP119 data. This should be a very good approximation for CYP119-I. Before we examine the CYP119 data and determine the spectrum of CYP119-I, we first illustrate the technique using the reaction of myoglobin (Mb) with peracetic acid.

The reaction of Mb with peroxides is known to yield ferryl myoglobin (compound II) in high yield. Although the generation of compound I precedes the formation of compound II, compound I does not accumulate appreciably in Mb.[51−53] As a result, the observation of Mb-I in wild-type enzyme is difficult at best. The situation is quite different in horseradish peroxidase, where compound I

(51) Matsui, T.; Ozaki, S.; Watanabe, Y. *J. Biol. Chem.* **1997**, *272*, 32735–32738.
(52) Matsui, T.; Ozaki, S.; Watanabe, Y. *J. Am. Chem. Soc.* **1999**, *121*, 9952–9957.
(53) Egawa, T.; Shimada, H.; Ishimura, Y. *J. Biol. Chem.* **2000**, *275*, 34858–34866.

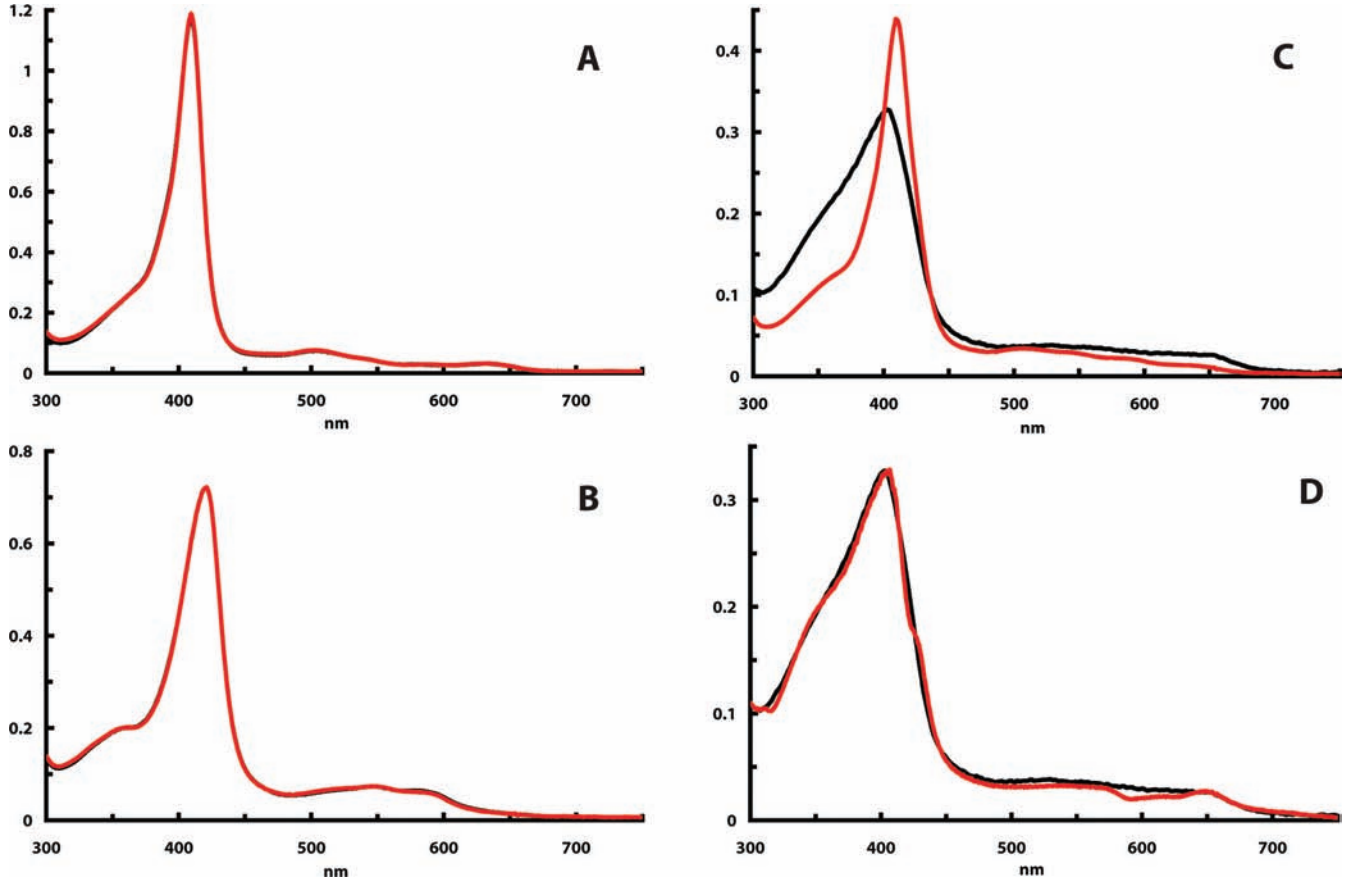

Figure 5. Target testing for Mb. Targeted vectors are shown in black, and the spectrum returned is in red. Target vectors are as follows: (A) ferric Mb; (B) ferryl myoglobin; (C) HRP-I; (D) HRP-I. Target testing in panel C was performed with two singular values. Target testing in panels A, B, and D was performed with three singular values.

(HRP-I) can be obtained in essentially quantitative yield.[54] Compound I in both systems is best described as an imidazole-ligated ferryl porphyrin radical. Thus, one expects very similar absorption spectra, and indeed work on His64 mutants of Mb has revealed that the UV/visible spectrum of compound I in the mutants is very similar to the spectrum of HRP-I.[51,52,54]

We now show that the spectrum of Mb-I can be obtained by target testing the spectrum of HRP-I on the stopped-flow data obtained for the reaction of Mb with peracetic acid. SVD of the Mb data set indicates three significant species in the reaction. The first four singular values are 122.7, 17.4, 1.04, and 0.10. Target test results are shown in Figure 5. Targeted spectra are in black, while those returned are in red. Panel A shows the results of target testing the spectrum of ferric Mb. The spectrum returned is essentially a carbon copy. The same is true in panel B for ferryl myoglobin (Mb-II). These species are an initial reactant and the final product of the reaction. Both are clearly visible in the reaction data, and one would certainly expect target testing to confirm that these species are present. What is not as clear-cut is the presence of Mb-I. As stated above, this species does not accumulate, and its presence cannot be readily detected by a visual examination of the stopped-flow data. Panels C and D show the results of target testing the HRP-I spectrum on the Mb data set. Panel C is pedagogical. It shows the results when only vectors corresponding to the first two singular values are retained for target testing. In this case, the spectrum returned does not resemble the spectrum of HRP-I. This makes sense because the two most important species in the data set are ferric Mb and Mb-II. The first two abstract vectors have only minor contributions from Mb-I, which is a fleeting species that contributes little to the data set. Panel D shows the results obtained when three singular values are retained. Target testing of the HRP-I spectrum now returns a spectrum that is remarkably similar to HRP-I and the Mb-I spectrum reported for His64 mutants. As stated above, this result indicates one of two things: (1) the projected spectrum is a good approximation of Mb-I or (2) the spectra of the three species in the reaction (i.e., ferric Mb, Mb-II, and Mb-I) can be added together to obtain a spectrum that is remarkably similar to the spectrum of HRP-I. As stated above, the second of these scenarios is highly unlikely.

We return to the UV/visible spectrum of CYP119-I. The second row of Figure 4 shows the results obtained when CPO spectra are target tested on the CYP119 data set. Targeting the spectra of ferric CPO (Figure 4D) and CPO-II (Figure 4E) returns vectors with no similarities to the targeted spectra. Again, this makes sense. SVD of the CYP119 data set indicates that only two species contribute significantly to the absorption data. These species are ferric CYP119 and CYP119-I, neither of which bears

(54) Dunford, H. B. *Heme peroxidases*; John Wiley: New York, 1999; p xiii, 507 p.

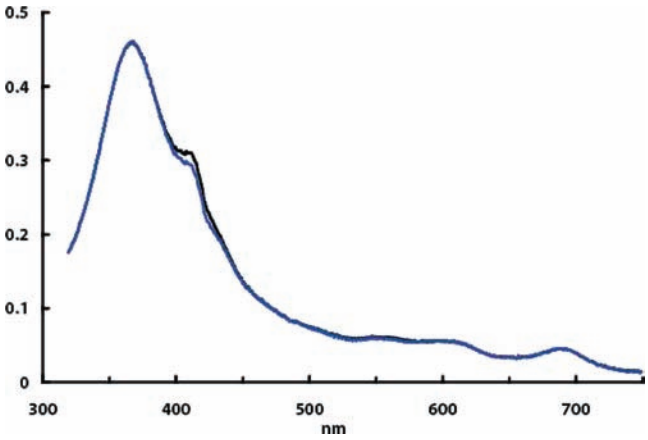

Figure 6. Comparison of CYP119-I spectra. The spectrum in blue was obtained from target testing of the CPO-I spectrum on the CYP119 data set. The black spectrum was obtained by manually combining abstract spectral vectors of the CYP119 data set.

any resemblance to ferric CPO (which is high-spin, λ_{max} = 400 nm) or CPO-II (λ_{max} = 438 nm). As a result, spectra resembling ferric CPO and CPO-II are not returned by target testing. Target testing of the CPO-I spectrum (Figure 4F) is different. The spectrum returned is similar to the spectrum of CPO-I and is virtually identical with the CYP119-I spectrum generated by manually combining the abstract vectors (Figure 6). The spectrum returned from the target testing of CPO-I is an excellent approximation of the CYP119-I spectrum.

Similar results are obtained when CYP119 spectra are target tested on the CPO data set. Nothing resembling (E) ferric CYP119 (low-spin) or (F) CYP119-NO emerges when these spectra are target tested. Targeting the spectrum of (F) CYP119-I, however, yields a spectrum with remarkable similarities: the spectrum of CPO-I.

Conclusion

We have generated the UV/visible spectrum of CYP119-I using two model-independent methods. Importantly, no assumptions about reaction kinetics were required to obtain the spectrum. The spectrum obtained closely resembles compound I spectra reported previously by Sligar and Egawa.[12,13] The spectrum of CYP119-I bears no resemblance to the putative P450-I spectrum obtained using LFP techniques.[6,7] One concludes that the LFP-generated intermediate is not P450-I.

This result is not unexpected. Compound I is two oxidizing equivalents above the ferric state: the suggestion that these species could have similar absorption spectra is an untenable position (see Figure 1 of ref 6). Additionally, the preparation of P450-I via LFP requires the production of P450-II. Newcomb has employed the reaction of PN with P450 to accomplish this task.[6−11,38] There is evidence that the reaction of PN with P450 yields a ferric nitrosyl complex.[39] It is not clear how compound I could be generated from such a species.

The LFP-generated species is not compound I. Its identity remains to be determined. Figure S1 of ref 7 may provide some insight. This figure reportedly shows the spectra of ferric CYP119, the PN-generated CYP119-II, and the LFP-generated CYP119-I. Although it is not expressly stated that these spectra are from the same reaction sequence, it appears that they are. If this is the case, it is telling that these three "distinct" species have multiple isosbestic points.

Interestingly, Newcomb and co-workers report kinetics, activation parameters, and kinetic isotope effects for reactions involving the LFP-generated species. The interpretation of these in light of our analysis is not straightforward. What is required is a thorough spectroscopic characterization of the LFP-generated species. Given the reported quantitative yields and exceedingly long lifetimes, the LFP-generated species would seem ripe for spectroscopic characterization. Mössbauer, electron paramagnetic resonance, and resonance Raman spectroscopies, in particular, would provide significant insights into the nature of the LFP-generated species. We await these spectroscopic reports.

Experimental Section

Materials. Peracetic acid (32%) was obtained from Fluka. *m*CPBA (<77%, Aldrich) was purified to 99% according to Davies et al.[55] Solutions of *m*CPBA were prepared by the addition of an acetonitrile stock. CPO was obtained from *Caldariomyces fumago* and purified (R_Z > 1.4) according to known procedures.[25] CYP119 (pCWori vector kindly provided by Paul Ortiz de Montellano) was overexpressed in BL21 cells and purified as reported previously.[42,56] An R_Z of >1.6 was used for all experiments. Equine metmyoglobin was purchased from Sigma and used without further purification. Protein used for stopped-flow experiments had an R_Z of 4.8.

Stopped-Flow Spectrophotometry. Spectral changes were monitored using an SFM-400 stopped-flow rapid-scan spectrometer (Bio-Logic SA, Claix, France). The minimum dead time of the instrument was 1.6 ms. An L7893 light source (Hamamatsu, Tokyo, Japan) and a TIDAS photodiode (J&M GmbH, Essingen, Germany) were used to collect absorption data. All experiments were performed at 4 °C. Spectral deconvolution was performed using the SVD technique. Spectral deconvolution via SVD and target testing were performed using a program written by Jarod Younker in Igor Pro (Wavemetrics, Inc., Lake Oswego, OR).

CPO Reaction. Protein (19 μM) in 100 mM potassium phosphate (pH 6.0) was mixed with a 15 μM peracetic acid solution containing ~1 mM ethanol. The ethanol served to suppress the formation of CPO-II. The decay of CPO-I was completed within 2 s. A total of 10 individual data sets were averaged for data analysis.

Mb Reaction. Protein (13 μM) in 200 mM potassium phosphate (pH 6.0) was mixed with a 5 mM peractic acid solution. The formation of Mb-II was complete within 3 s. A total of 20 individual data sets were averaged for data analysis.

CYP119 Reaction. Protein (18 μM) in 100 mM potassium phosphate (pH 7.5) was mixed with 10 μM *m*CPBA. The decay of CYP119-I was complete within 750 ms. No protein degradation was observed. A total of 10 individual data sets were averaged for data analysis.

Supporting Information Available: First, second, third, and fourth abstract concentration profile vectors and third and fourth abstract spectra obtained from SVD of stopped-flow data. This material is available free of charge via the Internet at http://pubs.acs.org.

(55) Davies, D. M.; Jones, P.; Mantle, D. *Biochem. J.* **1976**, *157*, 247–253.
(56) Maves, S. A.; Sligar, S. G. *Protein Sci.* **2001**, *10*, 161–168.